DOI: 10.21062/mft.2023.070 http://www.journalmt.com

Analysis of the Coating Delamination after Laser Beam Cutting

Anna Mičietová (0000-0003-4648-9975)[1], Miroslav Neslušan (0000-0001-7702-4578)[1], Zuzana Florková (0000-0001-9211-7537)[2], Mária Čilliková (0000-0003-1698-078X)[1]
[1]Faculty of Mechanical Engineering, University of Žilina, Univerzitná 1, 01026 Žilina. Slovakia. E-mail: anna.micietova@fstroj.uniza.sk; miroslav.neslusan@fstroj.uniza.sk; maria.cillikova@fstroj.uniza.sk;
[2]Research Centre, University of Žilina, Univerzitná 1, 01026 Žilina. Slovakia. E-mail: zuzana.florkova@uniza.sk

This paper analyses surface after laser beam machining with respect of surface height irregularities, residual stress state as well as microstructure on the low alloyed steel S 235. Surface after laser beam machining is investigated due to its specific nature resulting into coating delamination. This coating delamination can be found especially in the regions in which component shape or/and curvature of the profile is altered. Especially the components corners suffer from the delamination due to extensive surface heating and presence of brittle oxides layer. The thickness of this oxides layer is heterogeneous with respect of the component thickness as well as the component geometry. It was found the oxides layer is the thermally initiated process since in these regions the underlying matrix also exhibits the higher thickness of the heat affected zone and higher degree of the hardening expressed in term of HV0.1. Furthermore, also the compressive residual stresses exhibit higher amplitudes in the region remarkably affected by the thermal cycle.

Keywords: Laser beam machining, Oxidation, Delamination, Surface hardening

1 Introduction

Laser beam machining (LBM) or cutting is frequently employed technology applied for a variety of the real industrial applications. Laser technology is nowadays widely employed in the additive technologies and the convetional as well as the selective laser metling technologies are used [1]. Apart from other laser assisted processes such as laser peening [2, 3], laser assisted surface hardening [4], or laser bending [5], LBM can be used for cutting process [6]. LBM can be very beneficial in production of components made of different materials when components of complicated geometry are cut off from sheets. This process is very fast, easy to use and producing the components of acceptable quality especially in term of the height of surface irregularities as well as their precision. Certain disadvantage can be viewed in limited thickness of samples depending on the process assisted gas, cutting conditions as well as microstructure of the components. Components after LBM can be directly used for the subsequent welding process or some surfaces can be finished in order to improve components precision or/and remove the heat affected zone (HAZ). Thermal load might be harrmfull with respect of componnets functionality as it was reported earlier [7]. Thermal load was analzed by many experimental as well as numerical techniques [8]. HAZ after LBM is a product of thermal cycle when the surface undergoes the heating followed by the rapid self-cooling [9, 10]. Absence of mechanical contribution makes understanding of surface state after LBM easier as contrasted against the other machining process in which surface state is a function of thermal load and the superimposing contribution of stress state between cutting edge and produced surface.

Previous studies reported in this field clearly demonstrated that surface quality expressed in many terms is heterogeneous with respect of the path of laser beam through the sample thickness [11]. Height or irregularities as well as the thickness of HAZ in which initially soft surface is hardened by thermal cycles is less in the region in which the laser beam enters the component surface and increases along with increasing components thickness [11]. Degree of the surface hardening depends on the energy dissipated into the workpiece [12, 13]. Therefore, the cutting conditions take the strong role. Thermal load is also a function of cutting speed (relative speed of laser beam motion through a component surface). This speed together with the corresponding thermal load of surface can be kept constant on the straight lines. As soon as components of complicated geometry are produced, cutting speed in the regions in which the shape is altered (changing curvature, corners, etc.) the heat energy dissipated by the component is more. Some components after LBM operated in the aggressive environment have to be coated in other to prevent the surface damage. It was found that delamination of coating after LBM occurs mainly in the aforementioned regions in which the shape is

altered. In order to avoid such unacceptable delamination, the understanding of the reasons resulting into delamination should be reported. This study was initiated by coating delamination which occurs directly in the real production and analyses important aspects having the major role in this aspect.

2 Experimental conditions

Experiments were carried out on the low alloyed steel S 235 which is widely and commercially available steel of nominal yield strength 235 MPa (C 0.17%, Mn 1.4%, P 0.035%, N 0.12% in weight %). Due to the low C content this steel is composed of ferrite and isolated island of pearlite. The component as that illustrated in Fig. 1 was produced from the sheet of thickness 4 mm and the size 1000 x 2000 mm. Red arrow indicates the critical position in which coating delamination can occur. This component is a part of electric switchboard and after LBM the components undergoes spray coating. LBM was performed using TruLaser 3030 FIBER (laser power 4 kW, cutting distance 0.4 mm, cutting speed 30 m.min^{-1}).

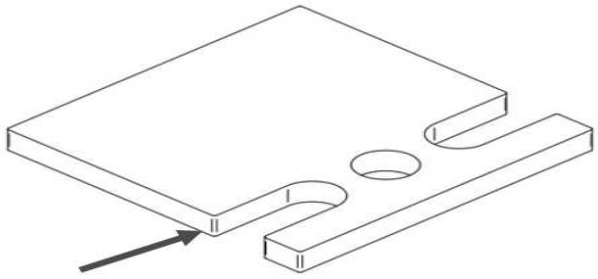

Fig. 1 *Component produced by LBM, size of component 60 x 60 mm (further information about components geometry kept secret)*

Samples after LBM were observed using the light microscope Zeiss AxioCam MRc5 in Olympus SZx16 and Quick Photo Industrial 3.0 software. Further observation and measurement of the height of surface irregularities was carried out using the laser confocal microscope Zeiss in software Zen (wavelength of the laser beam 405 nm, scanned area 3.5 x 3.5 mm, Z stack function). Residual stresses were measured along the laser beam direction. The XRD patterns were measured by Proto iXRD Combo (CrKα radiation in the plane {211}, sensing depth about 5 μm, scanning angles ± 39°, Bragg angle 156°, elastic constants for calculation of stresses ½s_2 = 5.75 TPa^{-1}, s_1 = −1.25 TPa^{-1}, collimator of the diameter 1 mm).

Also metallographic observations were carried out in region of laser beam entering into the sheet as well as on the trailing edge. The small specimens of the length 15 mm were cut by Secotom 50, hot moulded, ground, polished and Nital etched. Metallographic observations were carried out using Neophot 2 and software Niss Elements. The hot moulded samples were also employed for hardness measurement in order to quantify the degree of surface hardening and its extent to depth. HV0.1 was measured by an Innova Test 400TM (load of 100 g for 10 s). HV0.1 was obtained averaging by 3 repetitive measurements in the same depth.

3 Results of experiments

LBM produces the typically non-homogenous surface in which theee height of irregularities is increasing from the entering region towards the trailing edge, see Fig. 2. Moreover, it has been already reported that LBM also affects precision of produced parts [14]. In order to quantify these irregularities, the surface after LBM was scanned by the laser confocal microscope and 3D plot of the produced surface was obtained as that depicted in Fig. 3. This scan as well as the linear scans near by the entering and trailing edges as well as in the middle section (see Fig. 4 – 6 as well as Tab. 1) proves that the height of surface irregularities progressively grows from the entering towards the trailing edges. This grow is dramatic especially in the initial region of the laser path through the sample thickness and become less steep afterward. Fig. 2 and Fig. 3 demonstrate the typical wavy character of the cut surface after LBM. The height of the waves of higher wavelength dominates in the primary profile.

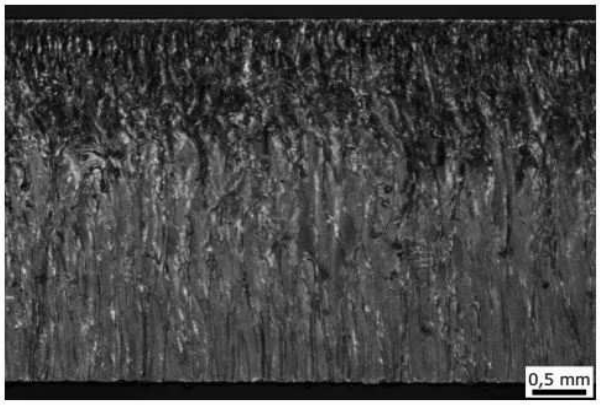

Fig. 2 *Large view of the surface after LBM, the light microscope Zeiss AxioCam MRc5 in Olympus SZx16*

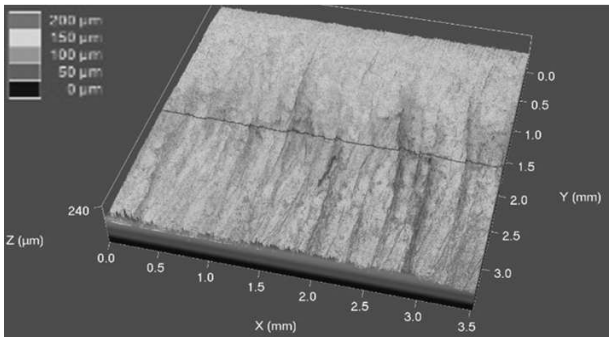

Fig. 3 *3D view of the surface irregularities (y axis along the sample thickness), laser confocal microscope Zeiss*

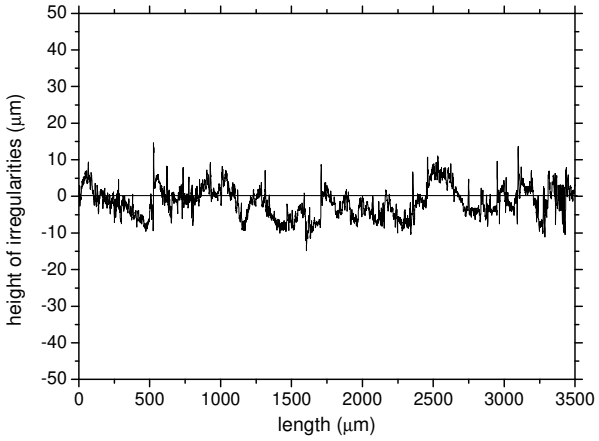

Fig. 4 *2D height of surface irregularities – entering region*

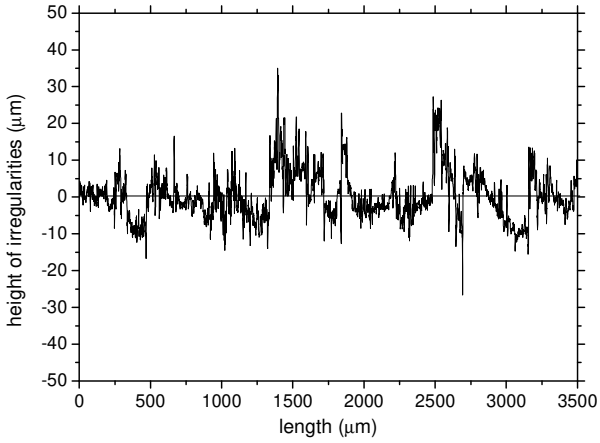

Fig. 5 *2D height of surface irregularities – middle region*

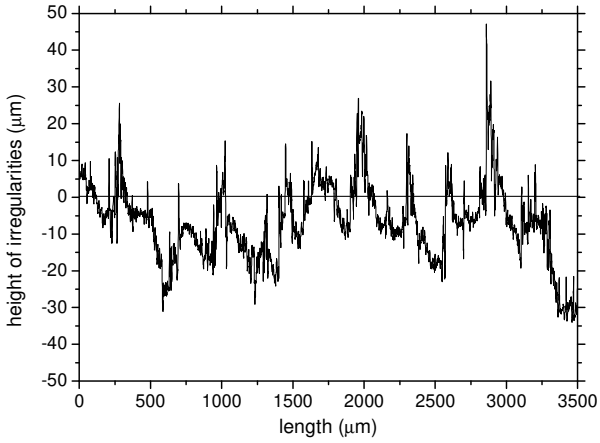

Fig. 6 *2D height of surface irregularities – trailing region*

Tab. 1 *Comparison of Pa and Pz values along the sample thickness*

	entering	middle	trailing
Pa, μm	3.9	5.2	7.9
Pz, μm	26.2	45.7	66.3
Pa - arithmetic mean deviation of the primary profile, Pz - maximum height of the primary profile			

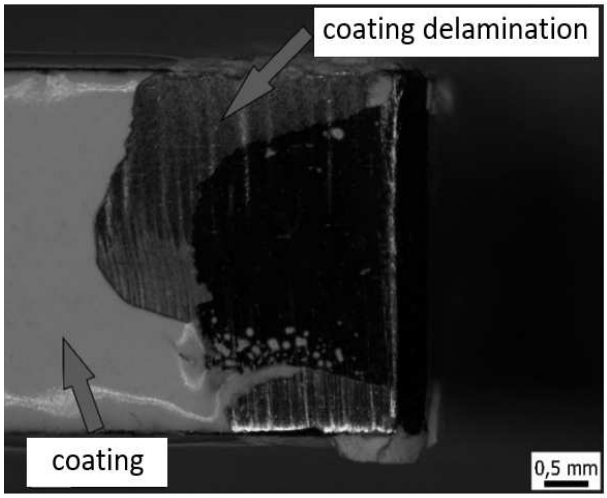

Fig. 7 *Coating delamination at the corner of the sample, the light microscope Zeiss AxioCam MRc5 in Olympus SZx16*

Quite rough surface after LBM takes certain role in the coating delamination as that depicted in Fig. 7. This figure demonstrates that this delamination can be mainly found in the sample corner. Position depicted in Fig. 7 links with the position indicated by the arrow in Fig. 1. Based on the further experience with staff operated by laser cutting machine, this delamination can occur in positions in which the component geometry is altered (changing curvature, corners, etc.). Measurement of residual stresses along the laser beam path indicates that the compressive stresses are produced as a result of thermal cycle, especially rapid self-cooling. However, the amplitude of these compressive stresses on the linear section of the components is - 160 ± 25 MPa whereas higher amplitude -257 ± 22 MPa can be measured near by the components corner. This information indicates higher degree of the heat entering the surface which can be proved the metallographic observation as that illustrated in Fig. 8. This figure clearly demonstrates that the thickness of HAZ which appears darker on the image is less in the linear region as that at the corner.

It is considered that the duration of thermal cycle is longer in the corner region due to process kinematics and the delays in the laser beam motion when the direction of the mutual motion is altered. Moreover, detail of the corner in Fig. 9 also depicts that the surface of the corner section contains the thin oxide layer which usually appears grey in metallographic images [15, 16]. Furthermore, the boundary between grey oxide layer and HAZ contains very thin white layer which is usually reported as the re-hardened very brittle martensite. On the other hand, the dark HAZ is referred as the rough martensite hardened by self-cooling followed after laser beam heating.

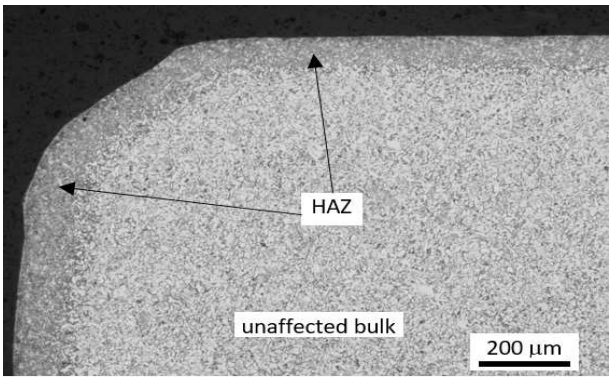

Fig. 8 *Metallographic image of HAZ after LBM, entering region*

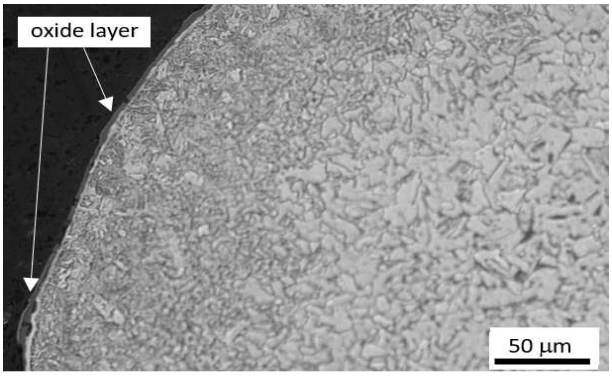

Fig. 9 *Metallographic image of HAZ after LBM, entering region, detail*

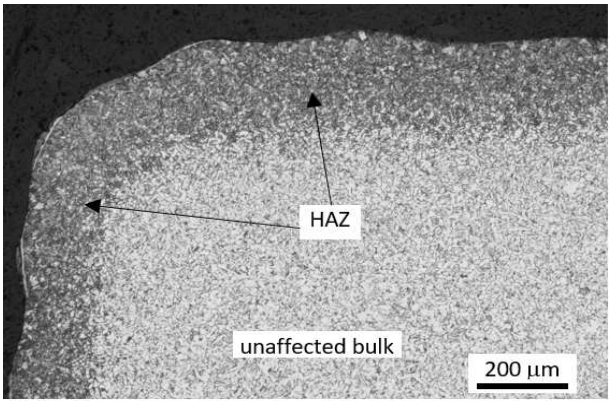

Fig. 10 *Metallographic image of HAZ after LBM, trailing region*

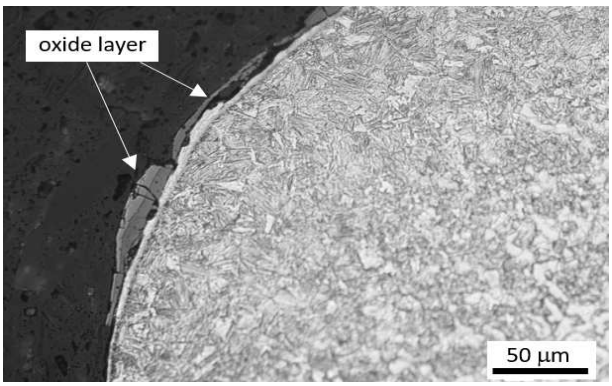

Fig. 11 *Metallographic image of HAZ after LBM, trailing region, detail*

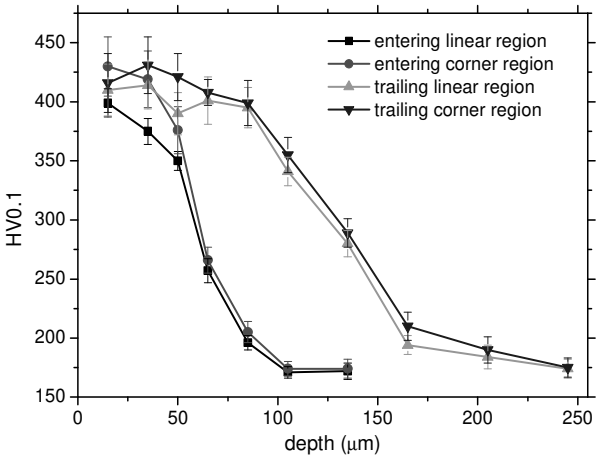

Fig. 12 *HV0.1 depth profiles in the different regions*

Fig. 10 depicts that the thickness of the HAZ at the trailing edge is more as that at the entering edge. Thickness of HAZ at the entering edge is about 0.1 mm and this thickness is approx. twice as higher at the trailing edge. Fig. 10 also proves the higher height of surface irregularities at the trailing edge as compared with the entering one. It can be clearly demonstrated that the surface on the metallographic image in Fig. 8 is more or less smooth and becomes remarkably wavy at the trailing edge. The detail of the trailing edge also demonstrates that the thickness of oxide layer as well as the white re-hardened layer are remarkably more as those at the entering edge.

Hardening effect on the component surface due to thermal cycle can be proved by the microhardness measurement HV0.1. This figure depicts that the degree of hardening at the entering and trailing edges is similar. However, its extent is more at the trailing edge which is consistent with the higher thickness of HAZ. The difference in HV0.1 profiles between the liner and the corner sections is only minor. Finally, the reasons of the coating delamination as that illustrated in Fig. 7 should be indicated. The main clue can be linked with Fig. 11 in which quite thick oxide as well as white re-hardened layer in found on the dark HAZ. These layers are quite brittle and hard [7, 10, 11] and can easily delaminated. Moreover, the oxide layer misses the direct contact with the underlying surface in many positions. Having sprayed coating as that depicted in Fig. 7, its delamination can be directly linked with presence of the thick oxide layer which occurs mainly on the components corners. Delamination of coating is therefore a result of the oxide layer poor contact with the underlying surface and its poor malleability. It is worth to mention that the oxide layer as well as white re-hardened layers occur on the linear region of component as well. However, these layers are discontinuous and their thickness is much lower as that found at the component corners.

4 Conclusions

Avoiding the coating delamination should be linked with the avoiding presence of thick oxide layer especially at the components corners. Two different strategies should be considered. First one is based on the reduction of heat entering the surface in these critical regions. Such approach can be linked with the alteration of LBM conditions such as laser power, cutting speed, etc. The second way can be viewed in avoiding Fe matrix oxidation by the use of application of suitable assisting laser gas. These strategies would also contribute to the better precision of produced components, elimination of residual stresses of higher magnitude as well as lower thickness of HAZ. Furthermore, it should be also noted that the increasing thickness of cut components will result into increased height of surface irregularities, higher thermal load which in turn means higher thickness of the oxide layer. Also component geometry should be considered as well. Especially the low angle passes might be critical. Matrix cooling in these positions would be delayed and thermal energy consumption increased with the negative role with respect of surface state.

Acknowledgement

This publication was realized with support of the KEGA project 010ŽU-4/2021 and VEGA project 1/0052/22.

References

[1] YANG, G., XIE, Y., ZHAO, S., REN, Y., WANG, CH. (2022). Methods and Mechanism of Powder Mixing for Selective Laser Melting. In: *Manufacturing Technology*, Vol. 22, No. 1, pp. 102-110. Czech Republic. ISSN: 1213-2489.

[2] PRAVEENKUMAR, K., SWAROOP, S., MANIVASAGAM, G. (2023). Effect of multiple laser shock peening without coating on residual stress distribution and high temperature dry sliding wear behaviour of Ti-6Al-4 V alloy. In: *Optics & Laser Technology*, Vol. 164, 109398. Germany. ISSN: 1879-2545.

[3] PROCHAZKA, J., VILIS, J., DOBROCKY, D., SPERKA, P. (2022). Modification of Diffusion Layers by Laser Shock Peening. In: *Manufacturing Technology*, Vol. 22, No. 6, pp. 724-732. Czech Republic. ISSN: 1213-2489.

[4] HRADIL, D., NOVÝ, Z., HODEK, J., KOUKOLÍKOVÁ, M., SZYSZKO, A. (2023). Effect of Laser Traverse Speed during Laser Hardening on Hardness Distribution and Microstructure of Hot Work Tool Steel H11. In: *Manufacturing Technology*, Vol. 23, No. 2, pp. 153-160. Czech Republic. ISSN: 1213-2489.

[5] YADAV, R., GOYAL, D.K., KANT, R. (2022). Multi-scan laser bending of duplex stainless steel under different cooling conditions. In: *CIRP Journal of Manufacturing Science and Technology*, Vol. 39, pp. 345-358. Switzerland. ISSN: 1755-5817.

[6] MIČIETOVÁ, A., ČILLIKOVÁ, M., NESLUŠAN, M. (2013). Influence of surface geometry and structure after non-conventional methods of parting on the following milling operations. In: *Manufacturing Technology*, Vol. 13, No. 1, pp. 199-204. Czech Republic. ISSN: 1213-2489.

[7] LI, W., RONG, Y., HUANG, Y., CHEN, L., YANG, Z., ZHANG, G. (2023). Effect of thermal damage on dynamic and static mechanical properties of CFRP short pulse laser hole cutting. In: *Engineering Fracture Mechanics*, Vol. 286, 109306. Netherlands. ISSN: 0013-7944.

[8] SLAMLOOEI, M., ZANON, G., VALLI, A., BISON, P., BURSI, O.S. (2022). Investigation of thermal behaviur of structural steel S235N under laser cutting process: Experimental, analytical, and numerical studies. In: *Engineering Structures*, Vol. 269, 114754. United Kingdom. ISSN: 0141-0296.

[9] KHDAIR, I.A., MELAIBARI, A.A., (2023). Experimental evaluation of cut quality and temperature field in fiber laser cutting of AZ31B magnesium alloy using response surface methodology. In: *Optical Fiber Technology*, Vol. 77, 103290. Italy. ISSN: 1068-5200.

[10] HUANG, S., FU, Z., LIU, CH., WANG, CH. (2023). Interactional relations between ablation and heat affected zone (HAZ) in laser cutting of glass fiber reinforced polymer (GFRP) composite by fiber laser. In: *Optics & Laser Technolgy*, Vol. 158, part A, 108796. Germany. ISSN: 1879-545.

[11] VAJDOVÁ, A., MIČIETOVÁ, A., ČILLIKOVÁ, M., NESLUŠAN, M. (2015). Barkhausen noise emission of surfaces after laser beam machining. In: *Manufacturing Technology*, Vol. 15, No. 3, pp. 462-468. Czech Republic. ISSN: 1213-2489.

[12] MIČIETOVÁ, A., ČILLIKOVÁ, M., ČEP, R., NESLUŠAN, M., GANEV, N. (2023). Study of Residual Stresses and Austenite Gradients in the Surface after Hard Turning as a Function of

Flank Wear and Cutting Speed. In: *Materials*, Vol. 16, 1709. Switzerland. ISSN: 1996-1944.

[13] WANG, J.Y., LIU, C.R. (1999). The effect of tool flank wear on the heat transfer, thermal damage and cutting mechanics in finishing hard turning. In: *CIRP Annals,* Vol. 48, pp. 53-58. USA. ISSN: 1726-0604.

[14] NADOLNY, K., ROMANOWSKI, M., SUTOWSKI, P. (2023). Assessing the technological quality of abrasive water jet and laser cutting processes by geometrical errors and a multiplicative indicator. In: *Measurement,* Vol. 217, 113060. United Kingdom. ISSN: 0263-2241.

[15] NESLUŠAN, M., BAHLEDA, F., MINÁRIK, P., ZGÚTOVÁ, K., JAMBOR, M. (2019). Non-destructive monitoring of corrosion extent in steel rope wires via Barkhausen noise emission. In: *Journal of Magnetism and Magnetic Materials,* Vol. 484, pp. 179-187. The Netherlands. ISSN: 0304-8853.

[16] PASTOREK, F., DECKÝ, M., NESLUŠAN, M., PITOŇÁK, M. (2022). Usage of Barkhausen Noise for Assessment of Corrosion Damage on Different Low Alloyed Steels. In: *Applied Sciences,* Vol. 11, 10646. Switzerland. ISSN: 2076-3417.